APPENDIX B

"PREDICTION OF EFFLUENT TEMPERATURES AND COMPOSITIONS FOR FIXED-BED COAL GASIFIERS"

Paper Submitted to Combustion Science and Technology

(Submitted to Combustion Science and Technology)

PREDICTION OF EFFLUENT TEMPERATURES AND COMPOSITIONS FOR FIXED-BED COAL GASIFIERS

M. L. Hobbs, P. T. Radulovic and L. D. Smoot[§]
Advanced Combustion Engineering Research Center
Brigham Young University, Provo, Utah 84602 (801) 378-4326

Keywords--Coal, effluents, equilibrium, fixed-bed, gasification, modeling

ABSTRACT

A two-zone, well-mixed, partial equilibrium model has been developed to provide efficient and accurate predictions of effluent temperatures and compositions from fixed-bed coal gasifiers. The model includes detailed treatment of devolatilization, partial equilibrium of volatile gases, treatment of a large number of gas phase species, and prediction of tar production with potential for recirculation of effluent products. Predictions have been compared to measured effluent temperatures and compositions from fixed-bed reactors. Quantitative agreement with experimental data has been obtained over a wide range of coal types. The model can be used separately or as part of a large process simulator since execution times are on the order of seconds. Furthermore, the predicted effluent temperatures and compositions can provide useful initial estimates for more complex one- or two-dimensional models.

INTRODUCTION

A schematic of a large-scale, fixed-bed gasifier is shown in Fig. 1. Coal is fed to the top of the reactor and moves downward under gravity, countercurrent to the rising gas stream. The dry ash is removed at the bottom of the reactor. The feed gas is composed of air or oxygen and steam. Excess steam is supplied to the gasifier to control the ash temperature. Figure 1 also shows the reactor divided into four overlapping zones: i) drying, ii) devolatilization, iii) gasification, and iv) combustion. As the coal slowly descends, the hot gases produced in the gasification and combustion zones exchange energy with the cooler solid fuel. Water and volatile matter are released when the solid reaches a sufficiently high temperature. After drying and devolatilization, the char enters the gasification zone where carbon reacts with steam, carbon dioxide and hydrogen. Endothermic reactions in this zone produce carbon monoxide and hydrogen. The slightly exothermic reaction of hydrogen with carbon produces methane. Differentiation between the "gasification zone" and the "combustion zone" can be made by the presence of free oxygen.

[§] The author to whom the correspondence should be directed

Heterogeneous combustion and gasification reactions can occur simultaneously in the "combustion zone". Combustible gases such as carbon monoxide or hydrogen react with gaseous oxygen. Solid residence time in the drying, gasification and oxidation zones may be on the order of several hours. Residence time in the ash layer may be even higher depending on the thickness of this zone. Gas residence times are on the order of seconds.

Gumz (1950) developed an equilibrium model for fixed-bed reactors. The effects of devolatilization, drying and sensible heat losses were not included in his model. Woodmansee (1976) extended Gumz's equilibrium model to include sensible heat losses. Kosky and Floess (1980) added devolatilization to the equilibrium model by assuming instantaneous devolatilization with yield based on proximate analysis and volatile composition based on the gas analysis of Loison and Chauvin (1964). Effluent temperatures were calculated using overall energy balances. Compositions where calculated assuming water-gas-shift equilibrium. Smoot and Smith (1985) have reviewed fixed-bed, fluidized-bed and entrained-bed models.

No major advancement has been made in predicting effluent temperatures and compositions in fixed-bed gasification in recent years. Even one- and two-dimensional, fixed-bed coal gasification models fail to predict accurate effluent properties. An assessment of the fixed-bed models of Amundson and Arri (1978), Yoon et al. (1978), Desai and Wen (1978), Stillman (1979), Cho and Joseph (1981), Yu and Denn (1983), Earl and Islam (1985), Thorsness and Kang (1986), and Bhattacharya et al. (1986) indicates common assumptions such as axially uniform gas/solid phase plug flow, uniform bed porosity, instantaneous devolatilization (with volatile yield from proximate analysis and composition assumed to be constant), char oxidation parameters from small particle data, and little or no gas phase chemistry. Recently, Hobbs et al. (1990) have relaxed most of these assumptions in a steady, one-dimensional model while emphasizing the importance of devolatilization and gas phase chemistry in fixed-bed gasification processes.

An efficient two-zone, partial equilibrium model has been developed and is presented in this paper. The two-zone, fixed-bed model uses a coal-independent devolatilization submodel and a partial equilibrium gas phase submodel to predict accurate effluent temperatures and compositions. Effluent compositions can be determined for any number of species. Tar production can also be predicted and tar recycle can be taken into account. In many engineering applications, only effluent temperatures and compositions are required. For example, only effluent information is required from the gasifier in a comprehensive process simulation used for optimization of the overall coal conversion process. Also, since simulation of the gasifier is often only a small part of complete process calculations, computational time must be kept to a minimum. In all such cases, the two-zone, partial equilibrium model is preferred to more complex and computationally demanding one- or two-dimensional models. Furthermore, the two-zone, partial equilibrium model can provide initial estimates for one- or two-dimensional models. Accurate initial estimates of fixed-bed reactor effluent temperatures and compositions have been found essential for solving the highly nonlinear, fixed-bed equation set (Hobbs et al., 1990).

TWO-ZONE, PARTIAL EQUILIBRIUM MODEL

Foundations and Assumptions

Typical temperature and concentration profiles in a large-scale, fixed-bed gasifier are illustrated in Fig. 1. Oxidation and gasification occur at relatively high temperatures compared to the cooler devolatilization zone. The temperature difference provides a natural division of the process into two zones. Higher temperatures in the oxidation/gasification section favor total equilibrium in the gas phase. Lower temperatures in the devolatilization zone favor partial equilibrium.

The primary assumption for the two-zone, partial equilibrium model is that the oxidation/gasification zone and drying/devolatilization zone can be assigned different temperatures, $T_{equilibrium}$ and T_{exit}, respectively. All gases are assumed to be in thermal equilibrium. Furthermore, the gases produced in the higher temperature oxidation/gasification zone are assumed to be in chemical equilibrium in this zone, but nonreactive in the lower temperature devolatilization/drying zone. The coal volatiles and water vapor produced in the lower temperature devolatilization/drying zone are also assumed to be nonreactive in this zone. Coals are assumed to be composed of various percentages of chemical functional groups (Solomon et al., 1988). Reactor geometry, operational parameters, heat loss or overall heat transfer coefficient, coal properties, coal burnout, and recycle tar fraction must be specified.

Energy Balance

Control volumes for three equilibrium model options are shown in Fig. 2. The one-zone models shown in Fig.'s 2a and 2b are included for comparison and show the evolution of the two-zone model. The energy balance around any control volume shown in Fig. 2 is:

$$\dot{m}_{s,in}h_{s,in} + \dot{m}_{g,in}h_{g,in} - \dot{m}_{s,out}h_{s,out} - \dot{m}_{g,out}h_{g,out} - Q = 0 \qquad (1)$$

where $\dot{m}$ ($\frac{kg}{s}$) and h ($\frac{J}{kg}$) refer to mass flow rate and total enthalpy, respectively. The subscripts *s*, *g*, *in* and *out* refer to solid, gas, entering control volume, and exiting control volume, respectively. The total equilibrium model shown in Fig. 2a assumes complete reaction of the dry, ash-free coal by either devolatilization, gasification or oxidation. The total equilibrium model does not differentiate among mechanisms for these chemical processes as do the one- and two-zone partial equilibrium models. The only difference between the one- and two-zone partial equilibrium models relates to devolatilization and drying. The one-zone model assumes that drying and devolatilization occur in the same zone as oxidation and gasification. This assumption is relaxed in the two-zone partial equilibrium model. Equation (1) can be solved by iteration. Total computation time for the two-zone partial equilibrium model is less than one second on an engineering workstation.

The total enthalpy is composed of the enthalpy of formation and the sensible enthalpy:

$$h = h_f^o + h^s \tag{2}$$

where the superscripts *o* and *s* refer to the reference temperature (298.15 K) and sensible enthalpy from the reference temperature to the stream temperature. The heat of formation of coal, $h_{f,c}^o$, is based on the following coal reaction:

$$C_nH_mO_hS_jN_k + \left(n + \tfrac{m}{4} - \tfrac{h}{2} + j\right)O_2 \rightarrow nCO_2 + \tfrac{m}{2}H_2O + \tfrac{k}{2}N_2 + jSO_2 \tag{3}$$

The heat of formation of the coal can be obtained from the higher heating value of the coal, HHV $(\frac{J}{kg})$, which can be measured or estimated from the ultimate analysis with Dulong's formula (Perry and Chilton, 1973). Therefore, the heat of formation of the coal is determined as the sum of the heats of formation of the products and the higher heating value of the coal:

$$h_{f,c}^o = \sum_{i=1}^{4} v_i h_{f,i}^o + HHV \tag{4}$$

where v represents the stoichiometric coefficient for the *i-th* product given in Eq. (3) and *i* represents the formation of CO_2, H_2O (l), N_2, and SO_2, respectively. Error results in calculating the heat of formation of coal, which is a relatively small number, as the difference of two much larger numbers of limited accuracy (Johnson, 1981). Fortunately, the enthalpy of the feed coal is small in comparison to the feed gas enthalpy for dry-ash, fixed-bed gasifiers and has little influence on the equilibrium calculations.

The heats of formation and sensible enthalpies for the feed gases are found with a generalized chemical equilibrium code (Pratt, 1985) which uses polynomial fits of data in the JANAF thermochemical tables (Stull and Prophet, 1971). The sensible enthalpy for the feed coal, h_c^s $(\frac{J}{kg})$, can be determined using Merrick's enthalpy correlation (1983) evaluated at 298.15 K and the coal feed temperature:

$$h_c^s = \left(\tfrac{R}{a}\right)\left[380g_o\left(\tfrac{380}{T}\right) + 3600g_o\left(\tfrac{1800}{T}\right)\right] \tag{5}$$

$$g_o(z) = \frac{1}{(\exp(z)-1)} \tag{6}$$

where R $(\frac{J}{kmol \cdot K})$ is the gas constant, 8314.4, T (K) is solid temperature, 380 and 1800 are characteristic Einstein temperatures, and z is a dummy variable representing the ratio of the Einstein temperature and T. The mean atomic weight, a, may be defined as:

$$\frac{1}{a}=\sum_{i=1}^{5}\frac{\Omega_i}{\mu_i} \qquad (7)$$

where μ_i represent the atomic weights of carbon, hydrogen, oxygen, nitrogen and sulphur, and Ω_i represents the dry, ash-free mass fractions of carbon, hydrogen, oxygen, nitrogen and sulphur obtained from the ultimate analysis. The specific heat of the ash, Cp_a ($\frac{J}{kg \cdot K}$), can be determined from (Merrick, 1983):

$$Cp_a = 754 + 0.586\,t \qquad (8)$$

where t ($^\circ C$) is the ash temperature.

The final term to define in Eq. (1) is the heat loss through the reactor wall, Q (*watts*). This quantity can be calculated if the jacket steam flow rate is known, or by the following equation if the overall heat transfer coefficient, U ($\frac{watts}{m^2 K}$), is known:

$$Q = UA(T_e - T_w) \qquad (9)$$

where A is the water wall surface area, T_e and T_w represent the well mixed exit temperature and the wall temperature, respectively. Values for the overall heat transfer coefficient, U, range from 50-200 $\frac{watts}{m^2 K}$ which is in the forced convection regime. Calculations herein use measured heat loss based on jacket steam flow rate.

Gas Phase Chemistry

Partial equilibrium allows certain reactions or species to be in chemical equilibrium while calculating other species by other means such as no reaction or kinetic rate controlled reaction. In other words, partial equilibrium for the mixture is assumed if any species is considered to be out of equilibrium. The species concentration may be found by assuming full equilibrium, by using heterogeneous kinetics (devolatilization, gasification, or oxidation), by using homogeneous gas phase kinetics, or by "freezing" the species to disallow further reaction. Most fixed-bed models in the literature have assumed the major gaseous species (CO, CO_2, H_2, and H_2O) to be in equilibrium, by the water-gas-shift reaction, while neglecting all minor species.

The approach taken herein is to allow major species to be in partial equilibrium or full equilibrium depending on the zone. Minor species are not neglected, but taken to be in equilibrium. Gas temperature is determined by assuming all gas species to be in thermal equilibrium even though chemical equilibrium may not exist. The equilibrium composition and temperature is determined by Gibb's free energy minimization (Pratt, 1985), given total gas phase static enthalpy, pressure and atomic composition.

The gases produced in the hot oxidation/gasification zone are assumed to be in complete equilibrium at the oxidation/gasification zone temperature. However, when these gases are cooled to the temperature of the drying/devolatilization zone, the oxidation/gasification zone gases are not allowed to react further. Also, the coal volatile gases and coal moisture produced in the cool devolatilization/drying zone are assumed to be nonreactive in the gas phase. In countercurrent fixed-bed gasifiers, these assumptions are justified by the low temperature of the drying/devolatilization zone which prevents further reactions of the volatile gases and coal moisture with the gases produced in the oxidation/gasification zone. The exit enthalpy or temperature is found by iteration using Eq. (1).

Devolatilization

Basis - Predicting accurate coal volatiles yield and composition is important since as much as 40-60 percent of the dry, ash-free mass can be lost by devolatilization. The primary difference between the total equilibrium model and the partial equilibrium models is the addition of yield computations for coal volatile matter. Devolatilization is assumed to take place instantaneously with the yield and composition equal to the ultimate volatile yield and composition. Large solid particle residence time, compared to the time required for complete devolatilization, justifies this assumption for this model of fixed-bed gasifiers. The ultimate volatile composition, including coal gas, tar and chemically-formed water yields, is predicted with a functional group model (Solomon et al., 1988).

The devolatilization submodel also predicts the amount and composition of the ultimate char fraction. Dulong's formula is used to calculate the heating value of the char which can be used to calculate the char heat of formation. Merrick's correlations (1983) are used to calculate the sensible enthalpy of the char. The tar fraction recirculated back to the oxidation/gasification zone is specified. The recirculated tar is assumed to react with the other gases in this zone to equilibrium. The gases, produced in the oxidation/gasification zone, and the coal volatiles and water vapor, produced in the devolatilization/drying zone, are assumed to be nonreactive in the devolatilization/drying zone.

Ultimate Composition - The coal particle shown in Fig. 3 is divided into various chemical functional groups. The X and Y values, shown in the two-dimensional description of the dry, ash-free coal, represent the chemical functional group components (Solomon and Hamblen, 1985). The Y dimension is divided into fractions according to the chemical composition of the coal. The X dimension represents non-tar-forming char, tar-forming char, and tar. The initial fraction of a particular functional group component is represented by y_i^o, and the sum of y_i^o's equals 1. The initial functional group components, y_i^o, and the potential tar-forming fraction, x^o, for five coals of interest here are given in Table 1. The coal-independent Arrhenius rate parameters for each functional group are also given in Table 1 (from Solomon et al., 1988).

The evolution of each functional group into the gas is represented by first order decay, $\frac{dy_i}{dt}=-k_i y_i$. The evolution of tar is described by the first order decay of the X dimension, $\frac{dx}{dt}=-k_x x$. Since the Arrhenius rate coefficients, k_i and k_x, are constant under isothermal conditions, y_i and x for volatile functional groups can be determined by integration: $y_i=y_i^o\exp(-k_i t)$ and $x=x^o\exp(-k_x t)$. Non-volatile functional group fractions are constant, $y_i=y_i^o$.

The fractional amounts of a particular functional group component that remain in the solid phase as char, or evolve as tar or gas, $\omega_{i,c}$, $\omega_{i,t}$, and $\omega_{i,g}$, can be determined by assuming that light gases do not evolve from the tar vapor (Solomon and Hamblen, 1985):

$$\omega_{i,c}=\left(1-x^o+x\right)y_i \tag{10}$$

$$\omega_{i,t}=\left(x^o y_i^o-xy_i\right)\frac{k_x}{k_i+k_x} \tag{11}$$

$$\omega_{i,g}=\left(1-x^o\right)\left(y_i^o-y_i\right)+\omega_{i,t}\frac{k_i}{k_x} \tag{12}$$

The ultimate volatile composition can then be determined by taking the limit of Eqns. (10), (11) and (12) as time becomes large and by accounting for the Arrhenius rate constants of non-volatile functional groups being zero, to give:

$$\omega_{i,c}^{\infty}=\begin{cases}0, & \text{for volatile functional groups}\\ \left(1-x^o\right)y_i^o & \text{for non - volatile functional groups}\end{cases} \tag{13}$$

$$\omega_{i,t}^{\infty}=\begin{cases}x^o y_i^o\frac{k_x}{k_i+k_x} & \text{for volatile functional groups}\\ x^o y_i^o & \text{for non - volatile functional groups}\end{cases} \tag{14}$$

$$\omega_{i,g}^{\infty}=\begin{cases}\left(1-x^o\right)y_i^o+x^o y_i^o\frac{k_i}{k_i+k_x} & \text{for volatile functional groups}\\ 0, & \text{for non - volatile functional groups}\end{cases} \tag{15}$$

The ultimate char composition, $\omega_{i,c}^{\infty}$, predicted by the functional group model, is not a function of temperature when the potential tar-forming fraction, x^o, is specified. However, the ultimate tar and gas compositions, $\omega_{i,t}^{\infty}$ and $\omega_{i,g}^{\infty}$, are functions of temperature even when x^o is specified because of the temperature-dependent Arrhenius rate constants, k_i and k_x.

Ultimate Yields - The ultimate char, tar, and gas yields, ω_c^{∞}, ω_t^{∞}, and ω_g^{∞}, are readily found from Eqns. (13), (14), and (15) by summing over functional groups:

$$\omega_c^{\infty}=\left(1-x^o\right)\sum_{i=in}y_i^o \tag{16}$$

$$\omega_t^{\infty} = x^o \sum_{i=iv} y_i^o \tfrac{k_x}{k_i+k_x} + x^o \sum_{i=in} y_i^o \tag{17}$$

$$\omega_g^{\infty} = \left(1-x^o\right) \sum_{i=iv} y_i^o + x^o \sum_{i=iv} y_i^o \tfrac{k_i}{k_i+k_x} \tag{18}$$

where the subscripts *iv* and *in* refer to volatile and non-volatile functional groups, respectively. The ultimate volatiles yield, ω_v^{∞}, is by definition a sum of the tar and the gas ultimate yields, ω_t^{∞} and ω_g^{∞}, and thus from Eqns. (17) and (18):

$$\omega_v^{\infty} = x^o + \left(1-x^o\right) \sum_{i=iv} y_i^o \tag{19}$$

The ultimate char yield, ω_c^{∞}, and the ultimate volatiles yield, ω_v, are not functions of temperature when the potential tar-forming fraction, x^o, is specified. However, the ultimate tar and gas yields, ω_t^{∞} and ω_g^{∞}, are functions of temperature because of the Arrhenius rate constants, k_i and k_x.

Potential Tar-Forming Fraction - The potential tar forming fraction, x^o, represents the maximum possible tar yield. However, competition from light gas evolution prevents maximum tar yield as shown in Eqns. (17) and (18). The potential tar-forming fraction can be adjusted to match experimentally determined tar yields, estimated from correlated experimental data (e. g. Kahn, 1989, Ko et al., 1988 and Serio et al., 1987), predicted from simple ultimate yield models (e. g. Kobayashi et al., 1977), or predicted from coal-structure-dependent models (e. g. Solomon et al., 1988). Values for the potential tar-forming fraction used herein were estimated from correlated experimental data (Serio et al., 1987) and are also given in Table 1. The tar recirculated back to the oxidation/gasification zone was specified to match the measured tar produced in the gasifier.

Arrhenius Rate Constants - Coal is viewed as a composite material consisting of a large number of component fractions with varying rates of decomposition. A multiple reactions model for each functional group (similar to that of Anthony et al., 1974) is used to distribute the Arrhenius rate constants. Here, it is assumed that the total volatile mass production from the *i-th* functional group is normally distributed to activation energy in the same manner as the total potential volatile mass production at large times. The resulting Arrhenius equation is:

$$k_i = \int_{-\infty}^{+\infty} k_i^o \exp\left(\tfrac{-E}{RT}\right) \frac{\exp\left[-\frac{1}{2}\left(\frac{E-\overline{E}_i}{\sigma_i}\right)\right]}{\sigma_i \sqrt{2\pi}} dE_i \tag{20}$$

Equation (20) was solved using seven point Gaussian-Legendre quadrature (Abramowitz and Stegun, 1972). Frequency factors, k_i^o, mean activation energies, $\overline{E}_i$, and standard deviations of activation energies, σ_i, were obtained from Solomon, et al. (1988) and are given in Table 1.

Oxidation and Gasification

Oxidation and gasification are treated by specifying char burnout percentage following devolatilization. Complete burnout was specified for the predictions herein. Large solid residence times and high oxygen concentrations and temperatures at the oxidation/gasification zone justify this assumption for fixed-beds. If more information is needed on carbon conversion, a one- or two-dimensional model with kinetic rates for oxidation and gasification is required (e. g., Hobbs et al., 1990).

EXPERIMENTAL DATA

Detailed experimental data on three high volatile bituminous coals and one subbituminous coal gasified in a high pressure, dry-ash, fixed-bed Lurgi gasifier in Westfield, Scotland, include flare gas analysis and gas offtake temperature (Elgin and Perks, 1973, 1974). The four coals are Illinois #6 (greatest reserve for Eastern caking coals), Illinois #5 (equivalent to Kentucky #9), Pittsburgh #8 (major Eastern coal with a high swelling index), and Rosebud subbituminous (from South-Eastern Montana). The Illinois #6 case has been used for comparison with several fixed-bed models (e.g. Yoon et al., 1978; Cho and Joseph, 1981; Kim and Joseph, 1983; Wen et al., 1982). Data for all four fixed-bed cases are given in Table 2.

Functional group data for Rosebud, Pittsburgh #8, and Illinois #6 coals gasified at Westfield are given in Table 1 (from Solomon et al., 1988 and Serio et al., 1987). Further, the properties of gasified Illinois #5 coal are taken to be those of Kentucky #9 coal in Table 1 since the two coals are reportedly from the same basin. The ultimate analyses corresponding to the functional group composition for these four coals is also given in Table 1. The ultimate analysis given in Table 1 and the ultimate analysis for the test coals in Table 2 differ, probably because the gasifier tests were performed several years ago and the analyses were based on different samples. Model results presented herein were calculated with the available functional group data and the corresponding ultimate analysis given in Table 1. Predictive results might have been improved if functional group data were available for the specific gasified test coals. In addition to these four coals, functional group data for North Dakota lignite used in the model sensitivity analysis are also included in Table 1. However, no gasification data were available for comparison with the lignite coal.

MODEL SENSITIVITY AND COMPARISONS WITH DATA

Sensitivity Analysis

Ultimate Volatile Distribution and Coal Gas Composition - Predicting accurate coal volatile distribution and coal gas composition is important since as much as 40-60 percent of the dry, ash-free mass can be lost by devolatilization. The predicted coal volatile distribution and composition is primarily dependent on coal rank, potential tar-forming fraction, and temperature.

A comparison of predicted ultimate volatile products distribution and coal gas composition for the five coals of Table 1 is shown in Fig. 4. The predictions are from Eqns. (15), (17) and (18) at 1000 K. In addition, distributions often assumed by other investigators are presented for comparison (e.g. the data of Loison and Chauvin, 1964, is used by Yoon et al., 1978, Kosky and Floess, 1980, Cho and Joseph, 1981, Yu and Denn, 1983). The ultimate volatile distribution and coal gas composition strongly depend on coal rank. The lower ultimate tar yields for lignites and subbituminous coals are consistent with expected values. The lower tar yields may be caused by crosslinking associated with CH_4 and CO_2 evolution (Solomon et al., 1988). The distribution of Loison and Chauvin (1964) should not be used for all coal types as is commonly assumed, but the coal volatiles distribution should be calculated for each coal rank. In fact, Yoon et al. (1978) assumed a different coal volatiles distribution than the Loison and Chauvin distribution for the Illinois #6 case to get reasonable predictions. Yoon's volatiles distribution used for Illinois #6 is also given in Fig. 4.

Predicted sensitivity of ultimate coal volatile products distribution and coal gas composition for Pittsburgh #8 to temperature and potential tar-forming fraction is shown in Fig. 5. The calculated tar yield is also shown. As much as 27% of the dry, ash-free mass of the coal may evolve as tar. In a fixed-bed, the tar may crack to form smaller light gas species or repolymerize to form char. The ultimate coal volatiles distribution is more sensitive to the potential tar-forming fraction than to the temperature. Furthermore, the coal gas composition is not very sensitive to either which emphasizes the importance of predicting accurate volatile distributions into tar, coal gas and chemical water as opposed to the coal gas composition. The lack of sensitivity of coal gas composition to the potential tar-forming fraction and temperature comes from competition between tar evolution and light gas evolution. When the tar rate constant, k_x, is significantly smaller than the light gas rate constant, k_i, then the sensitivity of the coal gas composition to both temperature and potential tar-forming fraction is small as seen from Eq. (15). This conclusion is supported also by experimental data (Blair et al., 1977, Solomon and Colket, 1979, Suuberg et al., 1979).

Temperature Sensitivity to Steam-to-Oxygen Ratio - The feed steam-to-oxygen ratio is often used to control ash temperature in a dry-ash, fixed-bed gasifier. Also, the steam-to-oxygen ratio affects the exit temperature and composition. The effect of the steam-to-oxygen ratio on the exit temperature of the three equilibrium model options for Illinois #6 coal, gasified in a commercial-scale Lurgi gasifier, is given in Fig. 6a. As expected, the exit temperature decreases with increasing steam flow rate. The temperature of the equilibrium zone predicted by the two-zone model is also shown. The one-zone exit temperatures are bounded by the two-zone exit and equilibrium temperatures. As the steam flow rate is increased, the differences among model options decrease.

Effluent Hydrogen-to-Carbon Monoxide Sensitivity to Steam-to-Oxygen Ratio - The effect of the steam-to-oxygen ratio on the exit molar ratio of hydrogen-to-carbon monoxide is shown in Fig. 6b. Data from various coals (Rudolph, 1972) are also shown for comparison. The operating conditions for the data of Rudolph were not given. Thus, quantitative agreement is not expected since the coals and operating conditions may not correspond. Qualitatively, all of the equilibrium model options predict the correct trend. Although the two-zone model gives better quantitative values for the hydrogen-to-carbon monoxide ratio, the predicted values are still higher than the measurements reported by Rudolph.

An implicit assumption in the ultimate volatiles prediction is that the composition of the tar is similar to that of the parent coal. This is a good assumption for high heating rates associated with entrained-bed gasifiers. However, Khan (1989) has recently shown an increase in hydrogen to carbon ratio in tar derived from fixed-bed reactors compared to entrained-bed reactors. The higher hydrogen content in the tar may be caused by increased secondary reactions due to increased residence time or prolonged contact with char. The sensitivity results and comparisons to measurements show that gaseous hydrogen is predicted too high. A possible explanation is the implicit assumption regarding the tar composition.

Fixed-Bed Effluent Data and Model Comparisons

Measured and predicted effluent temperatures and compositions are shown in Fig. 7 for Illinois #6, Pittsburgh #8, Illinois #5, and Montana Rosebud coals gasified in a high pressure, dry-ash, fixed-bed Lurgi gasifier at Westfield, Scotland. Measured and predicted tar, produced and recycled, are given in Table 2.

Tar Prediction - Predicted tar yields using the specified potential tar-forming fractions of 0.16 for a subbituminous coal and 0.43 for the three bituminous coals (Serio et al., 1987) were high in comparison to experimental measurements. Excess predicted tar was recycled to the oxidation/gasification zone and assumed to crack to produce light gases in equilibrium. Serio et al. (1987) imply that the potential tar-forming fractions are smaller for fixed-beds. This conclusion is consistent with the experimental measurements of Elgin and Perks (1974). A more rigorous method that depends on coal structure such as given by Grant et al. (1989), Solomon et al. (1988), Niksa (1988), or Niksa et al. (1987) is needed for better tar predictions. Also, fixed-bed experimental data are needed to find the optimum parameters for fixed-bed gasification.

Effluent Temperatures and Compositions - The measured effluent temperatures and compositions and those predicted for the total equilibrium, one-zone partial equilibrium, and two-zone partial equilibrium models are shown in Fig. 7. The Illinois #6 case also shows predictions from Yoon et al. (1978, one-dimensional model); these are probably the best predictions of effluent temperature and composition in the literature. The two-zone model predictions are as good as these predictions and better than the one-zone model predictions. Hydrogen predictions are high compared to measured values. High hydrogen predictions for gas may be a result of low hydrogen prediction for tar by the functional group model. Predicted carbon monoxide concentrations for both one-zone models are low, although the partial equilibrium model is closer to measured values. Carbon monoxide predictions from the two-zone model are closer to measured values. Other species are also predicted more closely to measured values with the two-zone partial equilibrium model.

The most interesting results are the Rosebud predictions. The one-zone models did not give reasonable exit temperature predictions or exit composition predictions for the Rosebud subbituminous coal case. The exit temperatures for the Rosebud, one-zone equilibrium predictions were as much as 230 K higher than measured values. The two-zone partial equilibrium model predicted the exit temperature for the Rosebud case to within 15 K. The energy required to dry the coal and heat up the feed coal causes the temperature in the drying/devolatilization zone to be lower. The predicted compositions for the Rosebud case with the two-zone partial equilibrium model were also in close agreement with measured compositions.

CONCLUSIONS

The two-zone, partial equilibrium model uses a coal-independent devolatilization submodel and a partial equilibrium gas phase submodel to predict effluent temperatures and compositions. Effluent compositions are determined for all the major species and a number of minor species. Tar production is predicted and tar recycle is taken into account.

The two-zone, partial equilibrium predictions demonstrate that the ultimate volatiles distribution and coal gas composition depend strongly on coal rank. The ultimate volatiles distribution is more sensitive to the potential tar-forming fraction than to the temperature. The coal gas composition is not very sensitive to either. This emphasizes the importance of predicting accurate volatiles distribution into tar, coal gas, and chemical water as opposed to the coal gas composition.

The predicted tar yields using the specified tar-forming fractions from the literature for various coal types are high in comparison to the values measured in commercial-scale, fixed-bed gasifiers. Also, the predicted hydrogen content in the tar seems to be low. A more rigorous method for predicting tar, probably one depending on coal structure, is needed.

The two-zone, partial equilibrium predictions compare well with experimental data for gasification of four coal types in a high pressure, commercial-scale, fixed-bed gasifier. Effluent compositions and temperatures are predicted with reasonable accuracy for a wide range of coal types by treating devolatilization/drying and char oxidation/gasification as two separate temperature zones. The hot oxidation/gasification gases favor total reaction equilibrium while the cooler devolatilization/drying zone gases favor partial equilibrium. Hydrogen predictions are high compared to measured values. High hydrogen in gas may be a result of low hydrogen in tar.

The two-zone, partial equilibrium model is preferred to more complex and computationally demanding one- or two-dimensional models when only effluent temperatures and compositions are required and computational times must be minimized as in large process optimizations. Furthermore, the two-zone, partial equilibrium model can provide accurate initial estimates for one- or two-dimensional models which is essential for the highly nonlinear gasification problem.

ACKNOWLEDGMENT

This work was sponsored principally by the U. S. Dept. of Energy/Morgantown Energy Technology Center (Contract No. DE-AC21-86MC23075, Richard Johnson, project officer) under subcontract from Advanced Fuel Research, Inc., East Hartford, CT. and also in part by the Advanced Combustion Engineering Research Center at Brigham Young University. Funds for this Center are received from the National Science Foundation (Tapan Mukherjee, project officer), the State of Utah, 25 industrial participants, and the U. S. Department of Energy. Consultations with P. R. Solomon and coworkers at Advanced Fuel Research are greatly appreciated.

REFERENCES

Abramowitz, M. and Stegun, I. A., eds., Handbook of Mathematical Functions With Formulas, Graphs, and Mathematical Tables, 10th printing, National Bureau of Standards, Applied Mathematics Series, 55, U. S. Government Printing Office, Washington, D. C. (1972).

Amundson, N. R. and Arri, L. E., "Char Gasification in a Countercurrent Reactor," AIChE J., 24, 87 (1978).

Anthony, D. B., Howard, J. B., Hottel, H. C. and Meissner, M. P., "Rapid Devolatilization of Pulverized Coal," 15th Symposium (International) on Combustion, The Combustion Institute, Pittsburgh, Pennsylvania, 1303 (1974).

Bhattacharya, A., Salam, L., Dudukovic, M. P. and Joseph, B., "Experimental and Modelling Studies in Fixed-Bed Char Gasification," Ind. Eng. Chem. Process Des. Dev., 25, 988 (1986).

Blair, D. W., Wendt, J. O. L., and Bartok, W., "Evolution of Nitrogen and Other Species During Controlled Pyrolysis of Coal," 16th Symposium (International) on Combustion, The Combustion Institute, Pittsburgh, Pennsylvania, 475 (1977).

Cho, Y. S., Joseph, B., "Heterogeneous Model for Moving-Bed Coal Gasification Reactors," Ind. Eng. Chem. Process Des. Dev, 20, 314 (1981).

Desai, P. R. and Wen, C. Y., "Computer Modeling of the MERC Fixed Bed Gasifier," MERC/CR-78/3, U. S. Department of Energy, Morgantown, West Virginia (1978).

Earl, W. B. and Islam, K. A., "Steady-state Model of a Lurgi-type Coal Gasifier," CHEMCA 85, paper c2b, 289 (1985).

Elgin, D. C. and Perks, H. R., "Results of Trials of American Coals in Lurgi Pressure-Gasification Plant at Westfield, Scotland," Sixth Synthetic Pipeline Gas Symposium, Chicago, Illinois, October 18-20 (1974).

Elgin, D. C. and Perks, H. R., "Trials of American Coals in Lurgi Pressure-Gasification Plant at Westfield, Scotland," Fifth Synthetic Pipeline Gas Symposium, Chicago, Illinois, October (1973).

Grant, D. M., Pugmire, R. J., Fletcher, T. H. and Kerstein, A. R., "Chemical Model of Coal Devolatilization Using Percolation Lattice Statistics," Energy & Fuels, 3, 175 (1989).

Gumz, W., Gas Producers and Blast Furnaces, Wiley, New York (1950).

Hobbs, M. L., Radulovic, P. T. and Smoot, L. D., "Chemical and Physical Processes in Countercurrent Fixed-bed Coal Gasification," submitted to the 23rd International Symposium on Combustion, Orleans, France (1990).

Johnson, J. L., "Fundamentals of Coal Gasification," in Chemistry of Coal Utilization, Second Supplementary Volume, M. A. Elliott, ed., John Wiley, New York (1981).

Khan, M. R., "A Literature Survey and an Experimental Study of Coal Devolatilization at Mild and Severe Conditions: Influences of Heating Rate, Temperature, and Reactor Type on Products Yield and Composition," Fuel, 68, 1522 (1989).

Kim, M. and Joseph B., "Dynamic Behavior of Moving-Bed Coal Gasifiers," Ind. Eng. Chem. Process Des. Dev., 22, 212 (1983).

Kobayashi, H., Howard, J. B. and Sarofim, A. F., "Coal Devolatilization at High Temperatures," 16th Symposium (International) on Combustion, The Combustion Institute, Pittsburgh, Pennsylvania, 411 (1977).

Ko, G. H., Sanchez, D. M., Peters, W. A. and Howard, J. B., "Correlations for Effects of Coal Type and Pressure on Tar Yields from Rapid Devolatilization," 22nd Symposium (International) on Combustion , The Combustion Institute, Pittsburgh, Pennsylvania (1988).

Kosky, P. G. and Floess, J. K., "Global Model of a Countercurrent Coal Gasifier," Ind. Eng. Chem. Process Des. Dev., 19, 586 (1980).

Loison, R. and Chauvin, F., "Prolyse Rapide du Charbon," Chem. Ind. (Paris), 91, 269 (1964).

Merrick, D., "Mathematical Models of the Thermal Decomposition of Coal. 2. Specific Heats and Heats of Reaction," Fuel, 62, 540 (1983).

Niksa, S., Kerstein, A. R. and Fletcher, T. H., "Predicting Devolatilization at Typical Coal Combustion Conditions with the Distributed-Energy Chain Model," Combustion and Flame, 69, 221 (1987).

Niksa, S., "Rapid Coal Devolatilization as an Equilibrium Flash Distillation," AIChE J., 34, 790 (1988).

Perry, R. H. and Chilton, C. H., eds., Chemical Engineers' Handbook, Fifth Edition, McGraw-Hill Book Company, New York (1973)

Pratt, D. T., "Multicomponent Equilibrium," in Pulverized-Coal Combustion and Gasification, eds. Smoot, L. D. and Pratt, D. T., Plenum Press, New York (1979).

Rudolph, P., "The Lurgi Process--The Route to S. N. G. From Coal," Proceedings of the Fourth Symposium of Synthetic Pipeline Gas, Chicago, Illinois (1972).

Serio, M. A., Hamblen, D. G., Markham, J. R. and Solomon, P. R., "Kinetics of Volatile Product Evolution in Coal Pyrolysis: Experiment and Theory," Energy & Fuels, 1, 138 (1987).

Smoot, L. D. and Smith, P. J., Coal Combustion and Gasification, Plenum Press, New York (1985).

Solomon, P. R., and Colket, M. B., "Coal Devolatilization," 17th Symposium (International) on Combustion, The Combustion Institute, Pittsburgh, Pennsylvania, 131 (1979).

Solomon, P. R. and Hamblen, D. G., "Pyrolysis," in Chemistry of Coal Conversion, ed. Schlosberg, R. H., Plenum Press, New York (1985).

Solomon, P. R., Hamblen, D. G., Carangelo, R. M., Serio, M. A. and Deshpande, G. Y., "General Model of Coal Devolatilization," Energy and Fuels, 2, 405 (1988).

Stillman, R., "Simulation of a Moving Bed Gasifier for a Western Coal," IBM J. Res. Develop., 23, 240 (1979).

Stull, D. R. and Prophet, H., JANAF Thermochemical Tables, Second Edition, National Bureau of Standards (1971).

Suuberg, E. M., Peters, W. A. and Howard, J. B., "Product Compositions and Formation Kinetics in Rapid Pyrolysis of Pulverized Coal--Implications for Combustion," 17th Symposium (International) on Combustion, The Combustion Institute, Pittsburgh, Pennsylvania, 177 (1979).

Thorsness, C. B. and Kang, S. W., "A General-Purpose, Packed-Bed Model for Analysis of Underground Coal Gasification Processes," UCID-20731, Lawrence Livermore National Laboratory, University of California, Livermore, California (1986).

Wen, C. Y., Chen, H. and Onozaki, M., User's Manual for Computer Simulation and Design of the Moving Bed Coal Gasifier, Final Report prepared for Morgantown Energy Technology Center, U. S. Department of Energy, DOE/MC/16474-1390, Morgantown, West Virginia (1982).

Woodmansee, E. E., "Modeling of Fixed Bed Gas Producer," Energy Communications, 2, 13 (1976).

Yoon, H., Wei, J. and Denn, M. M., "A Model for Moving-bed Coal Gasification Reactors," AIChE J., 24, 885 (1978).

Yu, W. and Denn M. M., "Radial Effects in Moving Bed Coal Gasifiers," Chemical Engineering Science, 38, 1467 (1983).

Figure Captions

Figure 1. Schematic of large-scale, high pressure countercurrent fixed-bed gasifier. Temperature and concentration profiles are for illustration only.

Figure 2. Control volume for A) 1-zone total equilibrium model, B) 1-zone partial equilibrium model, and C) 2-zone partial equilibrium model.

Figure 3. Schematic of coal particle with devolatilization model based on chemical functional groups (Solomon et al., 1988). The potential tar-forming fraction of the non-volatile carbon functional group evolves as tar. The non-tar-forming C and S organic groups evolve via heterogeneous char oxidation or gasification. (Figure from Hobbs, et al., 1990).

Figure 4. Comparison of coal volatiles distribution and ultimate coal gas composition for various coals. A) Ultimate gas distribution predicted from function group model at 1000 K and various maximum tar yields. Distributions from Loison and Chauvin (1964) and Yoon (1978) at unspecified conditions are also shown. B) Ultimate coal gas compositions at same conditions as shown in A.

Figure 5. Predicted sensitivity of coal volailes distribution and coal gas composition for Pittsburgh #8 to temperature and potential tar form fraction. A) Predicted sensitivity of ultimate volatiles distribution to potential tar forming fraction when temperature is constant at 1000 K. B) Predicted sensitivity of ultimate volatiles distribution to temperature when potential tar forming fraction is constant at 0.5. C) Predicted sensitivity of ultimate coal gas composition to potential tar forming fraction when temperature is constant at 1000 K. D) Predicted sensitivity of ultimate coal gas composition to temperature when ultimate tar forming fraction is constant at 0.5.

Figure 6. Temperature and composition sensitivity to steam-to-oxygen ratio. A) Predicted temperature sensitivity to steam-to-oxygen ratio for various equilibrium model options using Illinois #6 in Westfield gasifier. B) Comparison of the effect of steam-to-oxygen feed ratio on hydrogen-to-carbon monoxide ratio for several fixed-bed test results and various equilibrium model options. Comparison is with Rudolph (1972).

Figure 7. Comparisons of predictions and measurements for Westfield fixed-bed tests: A) Illinois #6, B) Pittsburgh #8, C) Illinois #5 (or Kentucky #9), and D) Montana Rosebud. Measurements are from Elgin and Perks (1974).

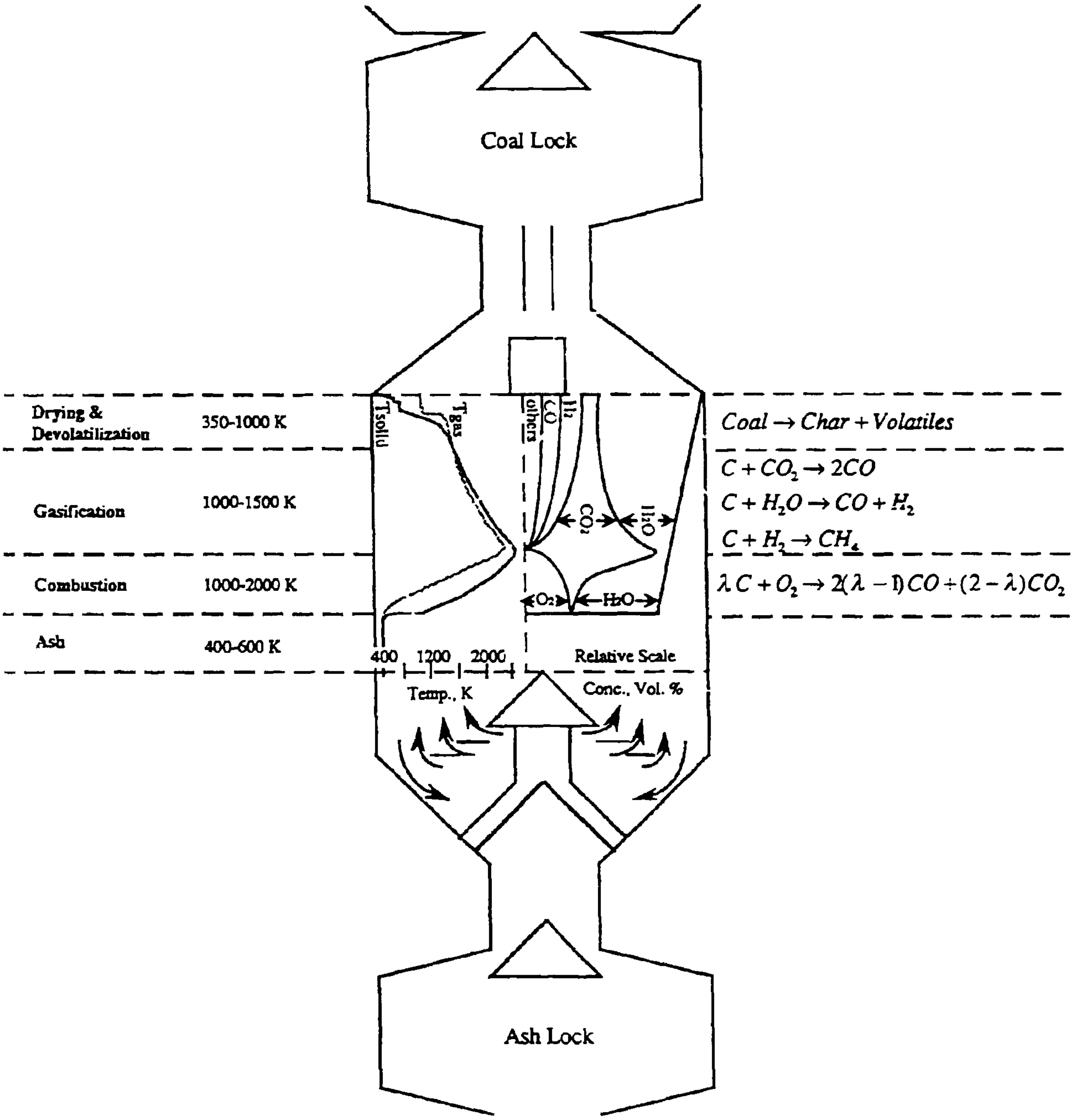

Figure 1. Schematic of large-scale, high pressure countercurrent fixed-bed gasifier. Temperature and concentration profiles are for illustration only.

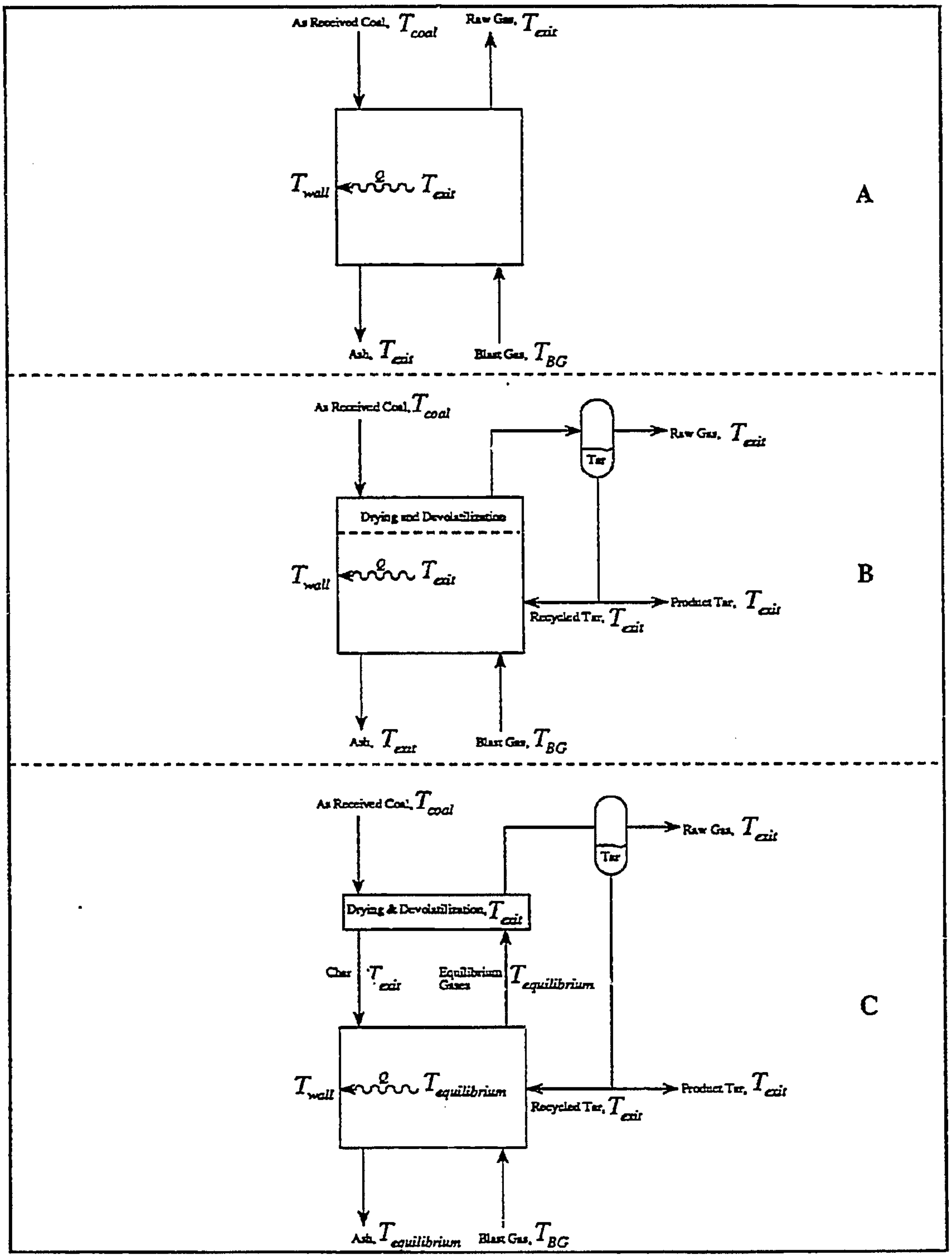

Figure 2. Control volume for A) 1-zone total equilibrium model, B) 1-zone partial equilibrium model, and C) 2-zone partial equilibrium model.

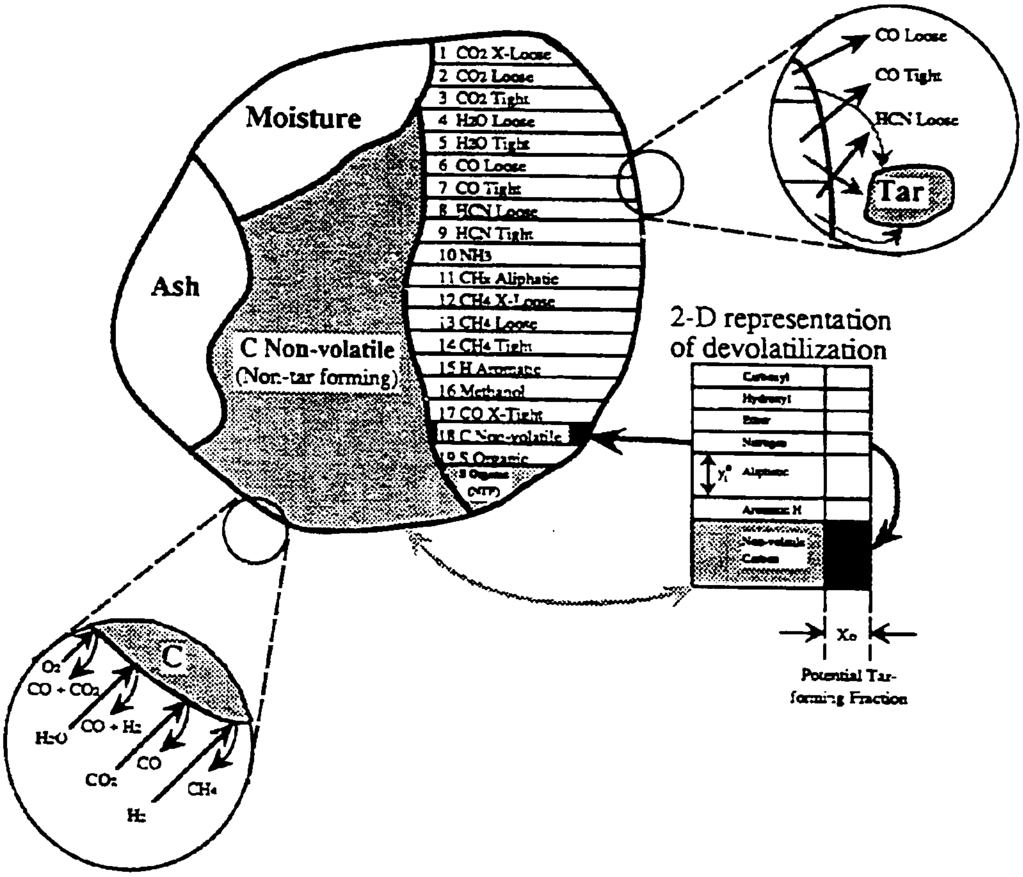

Figure 3. Schematic of coal particle with devolatilization model based on chemical functional groups (Solomon et al., 1988). The potential tar-forming fraction of the non-volatile carbon functional group evolves as tar. The non-tar-forming C and S organic groups evolve via heterogeneous char oxidation or gasification. (Figure from Hobbs, et al., 1990).

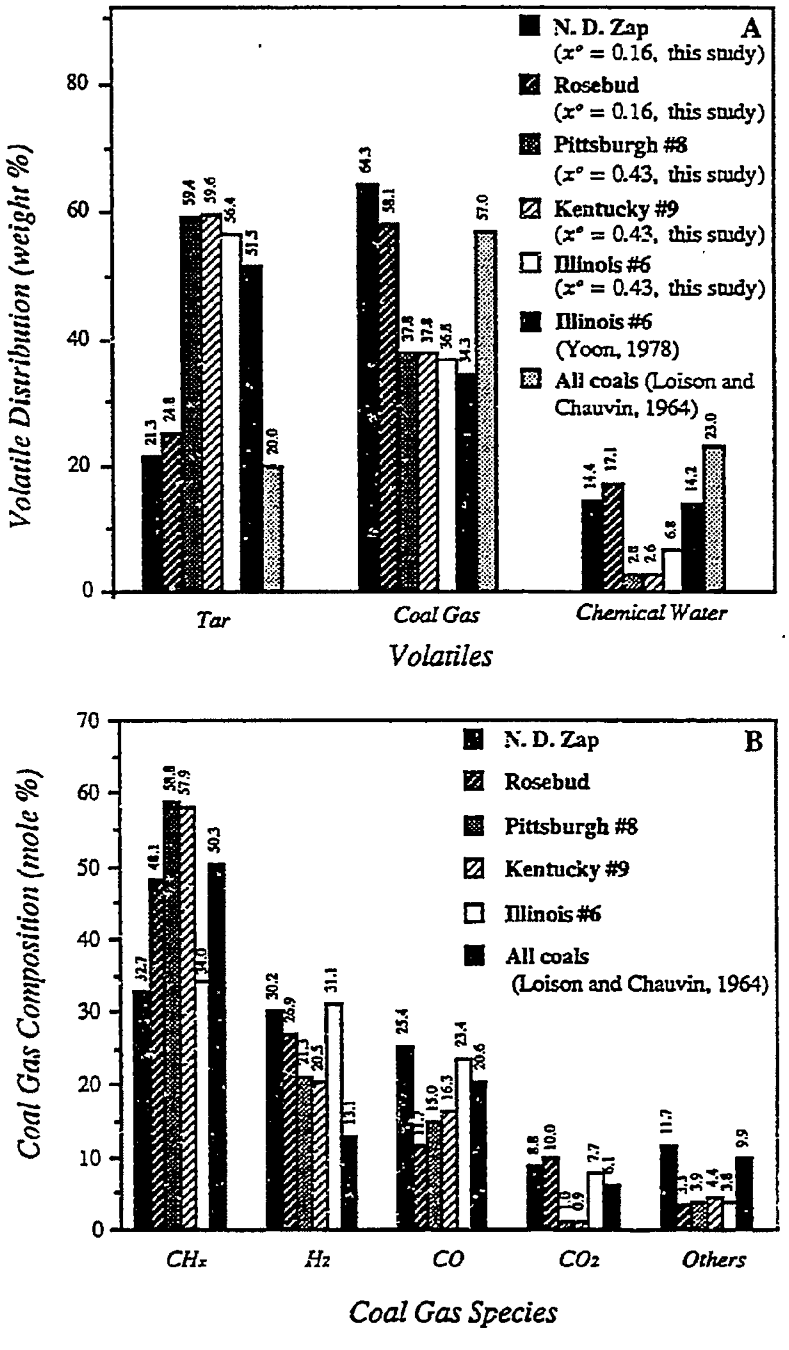

Figure 4. Comparison of predicted ultimate coal volatiles distribution and ultimate coal gas composition for various coals. A) Ultimate volatiles distribution predicted from functional group model at 1000 K and at various potential tar-forming fractions. Distributions from Loison and Chauvin (1964) and Yoon (1978) at unspecified conditions are also shown. B) Ultimate coal gas composition at same conditions as shown in A.

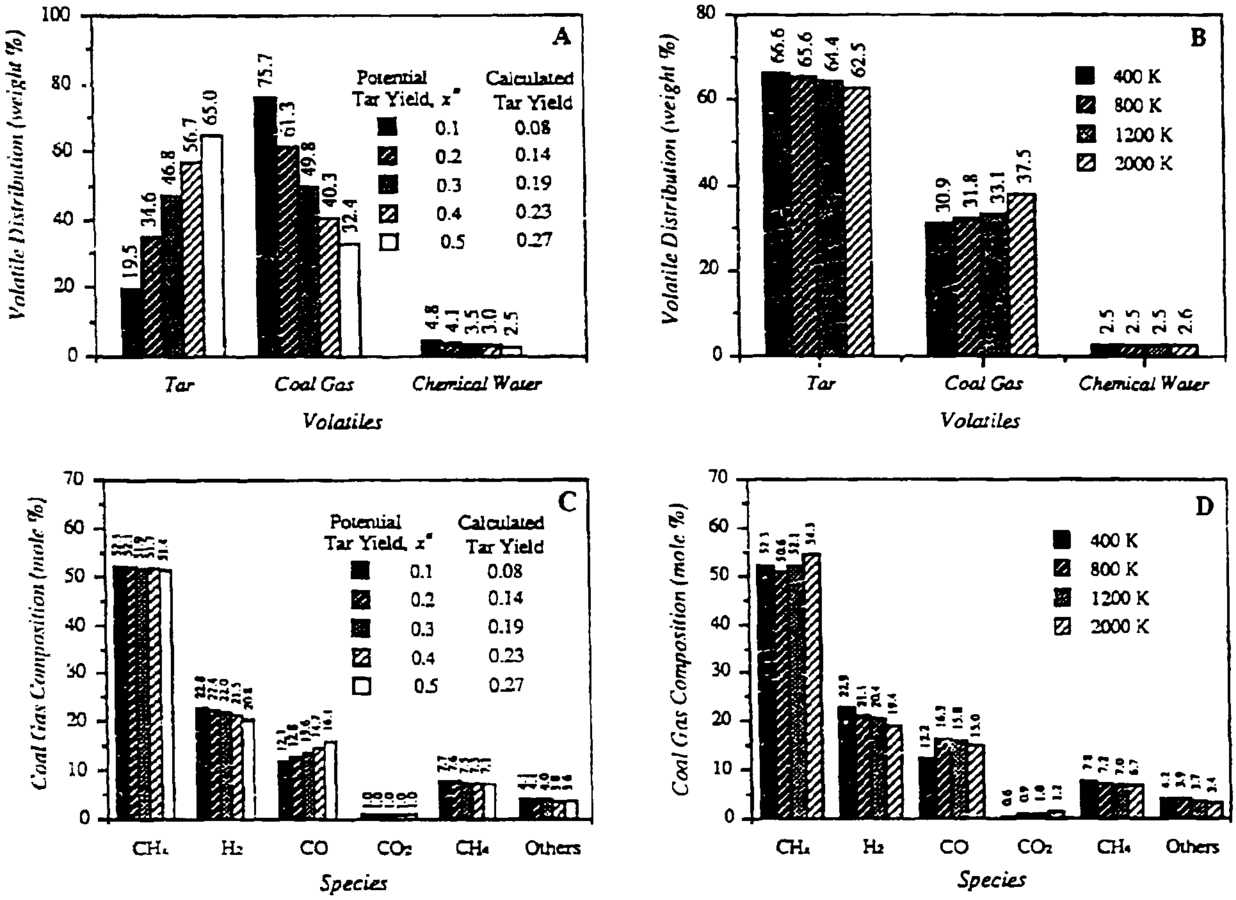

Figure 5. Predicted sensitivity of ultimate coal volatiles distribution and ultimate coal gas composition for Pittsburgh #8 to temperature and potential tar-forming fraction. A) Predicted sensitivity of ultimate volatiles distribution to potential tar-forming fraction when temperature is constant at 1000 K. B) Predicted sensitivity of ultimate volatiles distribution to temperature when potential tar-forming fraction is constant at 0.5. C) Predicted sensitivity of ultimate coal gas composition to potential tar-forming fraction when temperature is constant at 1000 K. D) Predicted sensitivity of ultimate coal gas composition to temperature when potential tar-forming fraction is constant at 0.5.

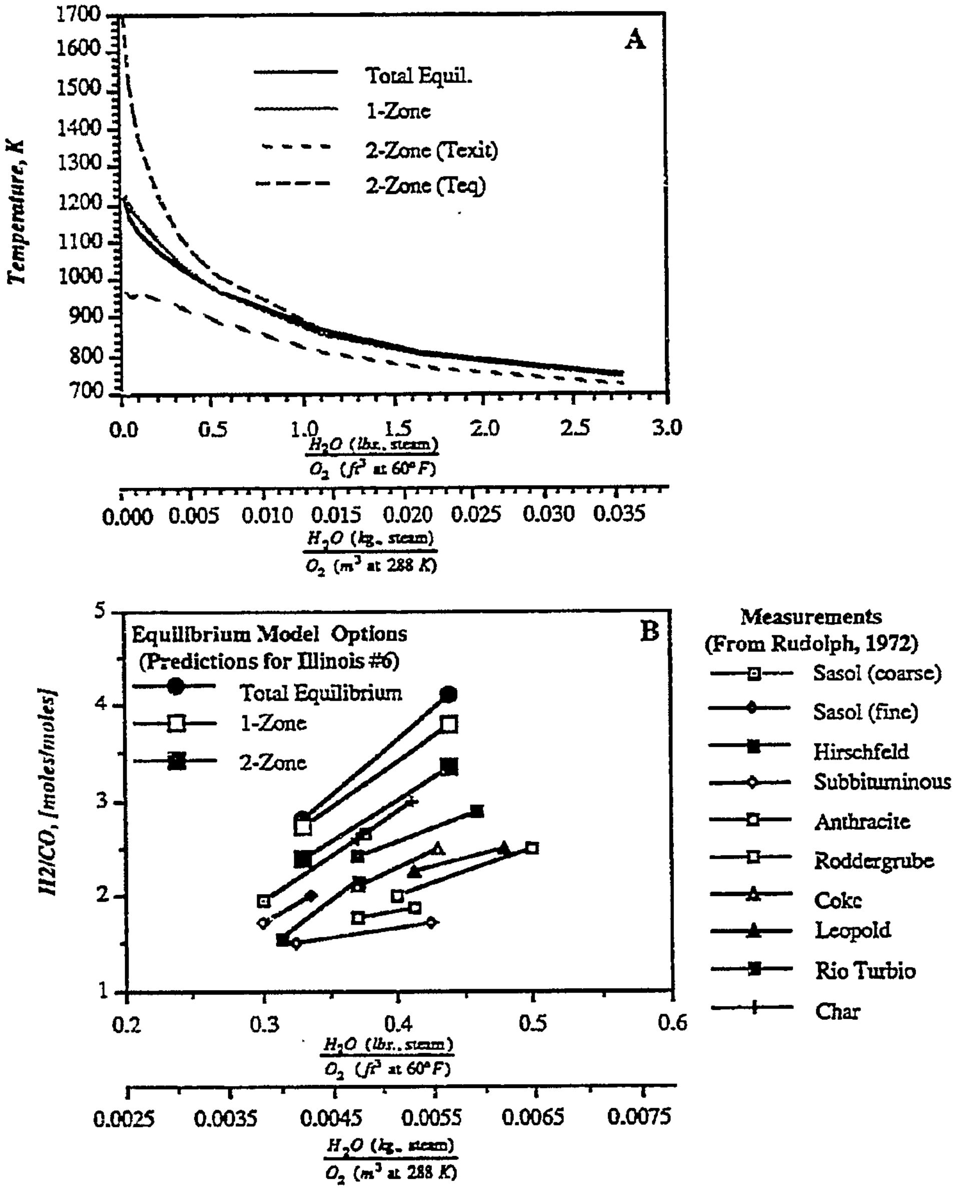

Figure 6. Temperature and composition sensitivity to steam-to-oxygen ratio. A) Predicted temperature sensitivity to steam-to-oxygen ratio for various equilibrium model options using Illinois #6 in Westfield gasifier. B) Comparison of the effect of steam-to-oxygen feed ratio on hydrogen-to-carbon monoxide ratio for several fixed-bed test results and various equilibrium model options. Comparison is with Rudolph (1972).

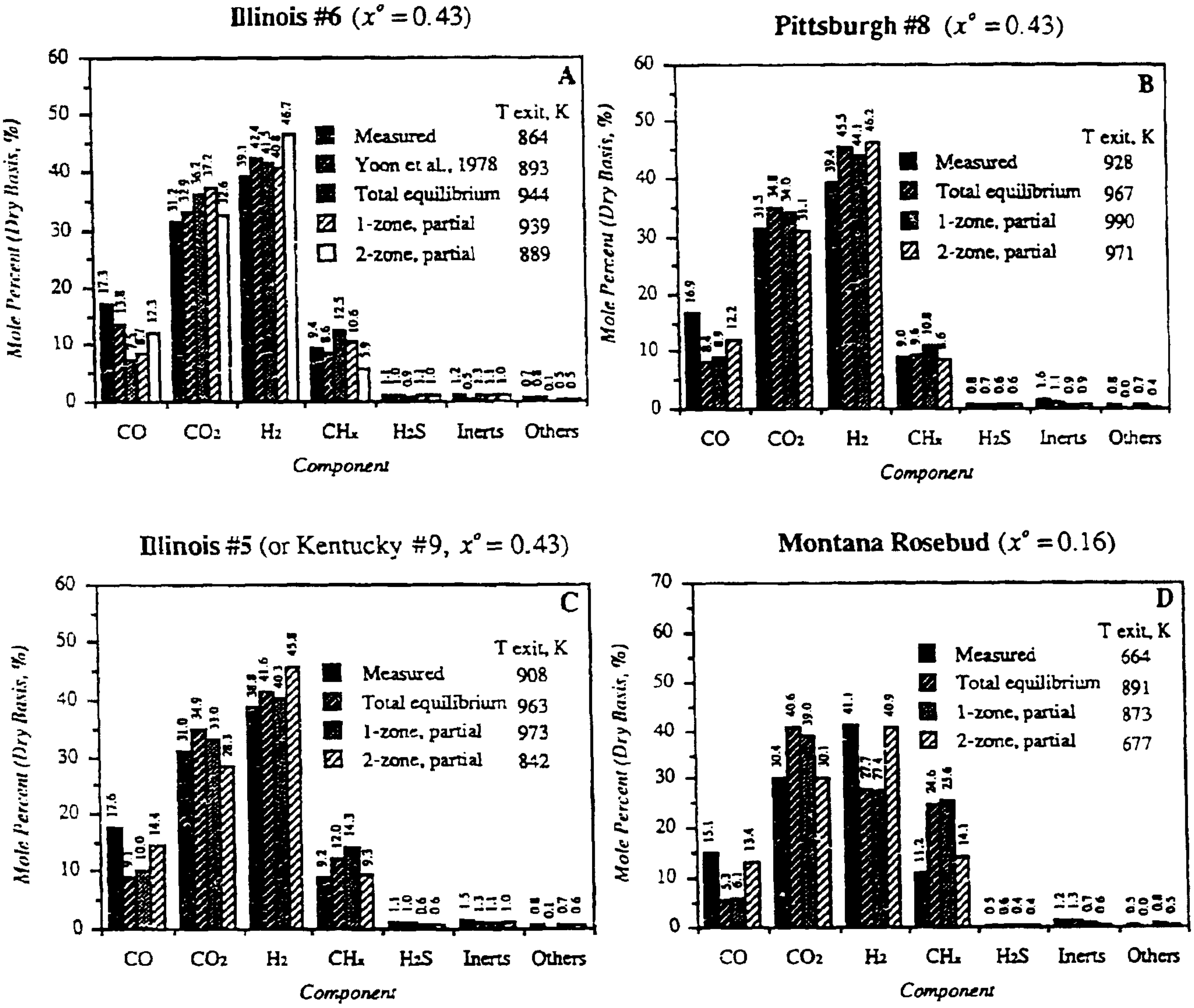

Figure 7. Comparisons of predictions and measurements for Westfield fixed-bed tests: A) Illinois #6, B) Pittsburgh #8, C) Illinois #5 (or Kentucky #9) and D) Montana Rosebud. Measurements are from Elgin and Perks (1974).

Table 1. Devolatilization parameters for ultimate volatile composition model from Solomon et al. (1988) and Serio et al. (1987)§.

Functional Groups (dry, ash free)	k_i^o, (s^{-1})	$\frac{E}{R}$, (K)	$\frac{\sigma}{R}$, (K)	**ND Zap,** y_i^o	**Rosebud** y_i^o	**Pitt #8** y_i^o	**KY # 9** y_i^o	**IL #6** y_i^o
CO_2 extra loose	0.81E+13	22500	1500	0.065	0.035	0.000	0.000	0.022
CO_2 loose	0.65E+17	33850	1500	0.30	0.035	0.007	0.006	0.022
CO_2 tight	0.11E+16	38315	2000	0.005	0.030	0.005	0.005	0.030
H_2O loose	0.22E+19	30000	1500	0.061	0.051	0.012	0.011	0.045
H_2O tight	0.17E+14	32700	1500	0.033	0.051	0.012	0.011	0.000
CO ether loose	0.14E+19	40000	6000	0.060	0.055	0.050	0.050	0.060
CO ether tight	0.15E+16	40500	1500	0.044	0.013	0.021	0.026	0.063
HCN loose	0.17E+14	30000	1500	0.006	0.005	0.009	0.026	0.10
HCN tight	0.69E+13	42500	4750	0.012	0.015	0.023	0.009	0.016
NH3	0.12E+13	27300	3000	0.001	0.001	0.000	0.000	0.000
CH_x aliphatic	0.84E+15	30000	1500	0.095	0.127	0.207	0.183	0.081
CH_4 extra loose	0.84E+15	30000	1500	0.000	0.000	0.000	0.020	0.011
CH_4 loose	0.75E+14	30000	2000	0.016	0.022	0.020	0.015	0.011
CH_4 tight	0.34E+12	30000	2000	0.009	0.012	0.015	0.015	0.022
H aromatic	0.10E+15	40500	6000	0.017	0.013	0.013	0.012	0.016
CH_3OH	0.00E+00	NA	NA	0.000	0.000	0.000	0.000	0.000
CO extra tight	0.20E+14	45500	1500	0.090	0.000	0.020	0.020	0.000
C nonvolatile	0.00E+00	NA	NA	0.440	0.520	0.562	0.562	0.550
S organic	0.00E+00	NA	NA	0.011	0.012	0.024	0.024	0.038
Total	NA	NA	NA	1.000	1.000	1.000	1.000	1.000
Tar, x^o	0.86E+15	27700	1500	0.160	0.160	0.430	0.430	0.430
DAF Ultimate Analysis								
C				0.817	0.724	0.821	0.817	0.736
H				0.056	0.049	0.056	0.056	0.047
N				0.019	0.012	0.017	0.019	0.014
O				0.084	0.203	0.082	0.084	0.165
S (organic)				0.024	0.012	0.024	0.024	0.038
Total				1.000	1.000	1.000	1.000	1.000

---

§ Data that is not applicable or not available is represented by NA

Table 2. Operating parameters and tar data for fixed-bed gasifier simulations.

Coal	Illinois #6	Illinois #5[*]	Pittsburgh #8	Rosebud
Type	Bituminous	Bituminous	Bituminous	Subbituminous
Proximate analysis, weight %				
Ash	9.1	8.1	7.7	9.7
Fixed carbon	46.0	44.7	50.3	36.4
Moisture	10.2	11.9	4.6	24.7
Volatile	34.7	35.2	37.4	29.2
Ultimate analysis, weight %				
Carbon	79.5	80.2	84.6	77.1
Hydrogen	5.4	5.4	5.8	4.9
Nitrogen	1.5	1.5	1.6	1.4
Sulfur	3.5	3.9	2.9	1.7
Oxygen	10.1	8.9	5.3	15.0
Operating Parameters				
Chamber diameter, m	3.66	3.66	3.66	3.66
Chamber length, m	3.05	3.05	3.05	3.05
Chamber pressure, KPa	2410	2450	2510	2560
Inlet coal temperature, K	370	370	370	370
Wall temperature, K	493	494	496	496
Coal mass flow, kg/s	1.67	1.80	1.02	2.23
Oxygen mass flow, kg/s	0.81	0.88	0.63	0.58
Steam mass flow, kg/s	4.20	4.04	3.29	2.80
Jacket steam mass flow, kg/s	0.89	0.73	0.66	0.31
Wall heat loss, megawatts	1.7	1.4	1.2	0.57
Predicted Tar Data[§]				
Product tar, kg/s	0.070	0.107	0.054	0.123
Recycle tar, kg/s	0.434	0.466	0.298	0.078
Total Tar, kg/s	0.504	0.573	0.352	0.201
Measured Tar Data[†]				
Product tar, kg/s	0.070	0.107	0.054	0.123
Recycle tar, kg/s	0.058	0.068	0.000	0.046
Total Tar, kg/s	0.128	0.175	0.054	0.169

---

[*] Illinois #5 coal is reported to be from the same basin as Kentucky #9 coal, and are taken to be equivalent coals.

[§] Predictions are from the two-zone, partial equilibrium model.

[†] Measurements are from Elgin and Perks (1974).

SATISFACTION GUARANTEED

NTIS strives to provide quality products, reliable service, and fast delivery. Please contact us for a replacement within 30 days if the item you receive is defective or if we have made an error in filling your order.

▶E-mail: info@ntis.gov

▶Phone: 1-888-584-8332 or (703)605-6050

Reproduced by NTIS

National Technical Information Service
Springfield, VA 22161

This report was printed specifically for your order from nearly 3 million titles available in our collection.

For economy and efficiency, NTIS does not maintain stock of its vast collection of technical reports. Rather, most documents are custom reproduced for each order. Documents that are not in electronic format are reproduced from master archival copies and are the best possible reproductions available.

Occasionally, older master materials may reproduce portions of documents that are not fully legible. If you have questions concerning this document or any order you have placed with NTIS, please call our Customer Service Department at (703) 605-6050.

About NTIS

NTIS collects scientific, technical, engineering, and related business information – then organizes, maintains, and disseminates that information in a variety of formats – including electronic download, online access, CD-ROM, magnetic tape, diskette, multimedia, microfiche and paper.

The NTIS collection of nearly 3 million titles includes reports describing research conducted or sponsored by federal agencies and their contractors; statistical and business information; U.S. military publications; multimedia training products; computer software and electronic databases developed by federal agencies; and technical reports prepared by research organizations worldwide.

For more information about NTIS, visit our Web site at **http://www.ntis.gov.**

NTIS

Ensuring Permanent, Easy Access to U.S. Government Information Assets

U.S. DEPARTMENT OF COMMERCE
Technology Administration
National Technical Information Service
Springfield, VA 22161 (703) 605-6000